IEEE Open Journal of Vehicular Technology

Received 19 May 2025; accepted 31 May 2025. Date of publication 9 June 2025;
date of current version 27 June 2025. The review of this article was coordinated by Editor Lei Zhang.

Digital Object Identifier 10.1109/OJVT.2025.3578224

Geographically Distributed Test Environment: Validation of Integrated Motion Control of Multi-Actuated Electric Vehicle

VIKTAR BELIAUTSOU [1], VIKTOR SKRICKIJ [2], JESÚS ALFONSO [3], JORIS GILTAY [4], FLORIAN BÜCHNER [1,5], JOSE ANGEL CASTELLANO [6] (Senior Member, IEEE), BARYS SHYROKAU [4], AND VALENTIN IVANOV [1] (Senior Member, IEEE)

[1]Technische Universität Ilmenau, 98693 Ilmenau, Germany
[2]Transport, Logistics Competence Centre, Vilnius Gediminas Technical University, 10223 Vilnius, Lithuania
[3]Mechatronics Department, Instituto Tecnológico de Aragón, 50018 Zaragoza, Spain
[4]Department of Cognitive Robotics, Delft University of Technology, 2628 CD Delft, The Netherlands
[5]EDAG Engineering GmbH, 85053 Ingolstadt, Germany
[6]Department of Computer Science, Systems Engineering, University of Zaragoza, 50018 Zaragoza, Spain

CORRESPONDING AUTHOR: VALENTIN IVANOV (e-mail: valentin.ivanov@tu-ilmenau.de).

This work was supported in part by European Community Horizon 2020 Framework Programme under Grant Agreement number 824333 and in part by the Research Council of Lithuania Project under Grant S-MIP-23-120.

ABSTRACT As an example of a geographically distributed test environment, an integrated motion control system for multi-actuated electric vehicles has been proposed and evaluated. This system unifies three active subsystems: drive-by-wire propulsion with independent in-wheel electric motors, electro-hydraulic brake actuators, and active suspension actuators. A distributed X-in-the-loop network architecture supports the approach, integrating a real-time validated vehicle model, dedicated test benches for each subsystem, and a driving simulator located in different geographical locations. This setup enables real-time testing and validation of the integrated control strategy. Validation results show improved ride comfort and safety.

INDEX TERMS Active suspension, electric vehicle, geographically distributed test environment, integrated motion controller, in-wheel motor, X-in-the-loop.

I. INTRODUCTION

Complex design tasks often necessitate comprehensive validation procedures using multiple experimental devices, and it is not always guaranteed that all required equipment will be available at a single location or owned by the same entity. A novel experimental testing methodology based on the real-time connection of test benches, which may be situated in different geographical locations and are united in a global X-in-the-loop (XIL) environment, was proposed several years ago [1]. A geographically distributed XIL methodology offers significant benefits for researchers by enabling the real-time coupling of various test benches from different locations. This paper contributes to and expands research in this area. For the case study, the integrated motion control (IMC) of a multi-actuated electric vehicle (EV) has been investigated.

The first comprehensive concept of IMC of multiple vehicle chassis and powertrain subsystems appeared in the mid-1980s [2]. The aim was to achieve a simultaneous improvement in the various performance characteristics of an EV, such as safety, energy efficiency, and ride comfort. However, the widespread market introduction of integrated vehicle dynamics/vehicle motion control systems has long been hampered by numerous technological obstacles related to total cost, computational effort, and actuator technology. However, advances in compact mechatronic components, chassis electrification, and the shift from individual control units toward high-performance computing led to the appearance of software-defined vehicles and new intensive research and industry studies on this topic.

When designing an IMC system, two important development tasks are considered independently of the control method to be used. The first task answers the question *"How much integration is enough integration?"*. When multiple systems, e.g. brakes, active suspension (AS), active steering,

in-wheel motor (IWM), active aerodynamics, wheel positioning, and tire inflation pressure, are available for coordinated control, it is necessary to select the proper integration level of all these systems and make their prioritization [3]. The second task relates to the development of an appropriate validation approach [4]. Integration can cause complex interference phenomena that can hardly be identified in a simulation environment during the design phase before the system is tested under real-world conditions using a vehicle demonstrator. A common example is the coupled influence of thermal processes in friction brakes and IWMs of an EV by considering brake blending [5] in the context of an IMC. Both these tasks are discussed in the presented paper.

It should be noted that it is based on the previous study of authors introduced in [6]. The primary gap in current IMC research is the predominance of simulation-based methodologies. This paper addresses this gap by proposing a hardware-based approach, offering a more direct and potentially more accurate investigation method. The contributions of the paper can be summarized as follows:

- The geographically distributed XIL network architecture is developed based on hardware components located across different locations. Real-time and synchronous performance of individual software and hardware components is ensured.

- The validation procedure of the proposed IMC for multi-actuated EVs is demonstrated.

The rest of the paper proceeds as follows. Section II provides an overview of the current state of the art. Section III outlines the use of a geographically distributed XIL test environment. In Section IV, the mathematical model of the vehicle is detailed. Following this, the proposed IMC is introduced and evaluated using the model-in-the-loop (MIL) approach, and the methodological approach is presented for validating integrated controls through XIL. Finally, the paper concludes with an analysis of the results.

II. RELATED STUDIES

IMC systems vary in complexity and are designed to improve EV dynamics performance in different ways: longitudinal, longitudinal with lateral, longitudinal with vertical, lateral with vertical, or across longitudinal, lateral, and vertical dimensions [7].

In initial studies, IMC demonstrated better utilization of tire friction, for example, with simultaneous operation of brake/traction control and active steering and active stabilizer, differential, and steering systems [8], [9], [10]. Later, it was also observed that the integration of the AS and the four-wheel steering system improves the lateral dynamics of the vehicle [11]. Therefore, integration may involve many vehicle systems in various combinations, which have been thoroughly analyzed in relevant studies such as [12], [13].

Most of the published studies on IMC systems aim to improve vehicle comfort, stability, and handling. Common solutions in this respect can be the combined operation of active steering together with wheel drive and/or brake torque control [14], [15], [16]. Further inclusion of AS can have a positive effect not only on ride quality but also on the lateral dynamics of the vehicle, as demonstrated in [17] and [18]. The approach discussed here is also of relevance for the verification and validation of automated driving functions with emulation of complex infrastructures, as shown in [19]. More recently, IMC has also been used for advanced applications related to automated driving tasks, e.g. to improve path following in addition to other driving dynamic features [20], [21], [22].

Regarding the control methods used in the known configurations of IMC systems, it can be stated that there are no established techniques that offer clear advantages over competing approaches. From the point of view of real-time applicability, rule-based integration can be advantageous. Such rule-based methods could, for example, be based on the activation thresholds for one or the other vehicle system depending on the maneuver type [23] or on the reference values for corresponding vehicle dynamics parameters [24]. However, distributing the overall control demand among the individual vehicle systems in order to simultaneously improve several vehicle characteristics (stability, comfort, etc.) can be a complex optimization task that requires advanced control allocation methods. In recent years, more attention has been paid to nonlinear methods such as sliding mode [25], [22] and especially model predictive techniques [26], [27], [28], [29], [30]. The complex architecture of the IMCs brings many challenges for validation procedures. It can be seen from the fact that the most cited references have investigated the controller functionality, mainly in simulation environments. By considering a common development process - from modelling to hardware-in-the-loop (HIL) testing and real vehicle experiments - the HIL phase has several specific aspects and is of particular interest in this study. In particular, it is hardly possible to install all components of the vehicle systems involved in IMC on the same HIL platform. It can become even more critical in industrial development, where the systems to be integrated may come from different suppliers.

A possible solution here can be the networking of several HIL platforms or component test benches in order to organize a synchronized real-time experiment. Such an approach has led to a number of studies over the last decade proposing the so-called remote and distributed XIL testing methodology, in which multiple participating experimental devices can be connected via a local area network or the internet, even if they are in different geographical locations [31], [32], [33], [34], [35].

A corresponding XIL variant was designed in which the driver simulator is connected with the driving IWM and dynamometer test bench setup to carry out bidirectional tests between Germany and China [36]. Another variant of distributed XIL aimed at powertrain control design is given in [37], where several prototype powertrain components are involved in real-time system simulation via an internet connection.

Despite the advantages arising from the XIL testing method, there are some critical aspects, such as time delays in data exchange, network-induced jitter, latency and data

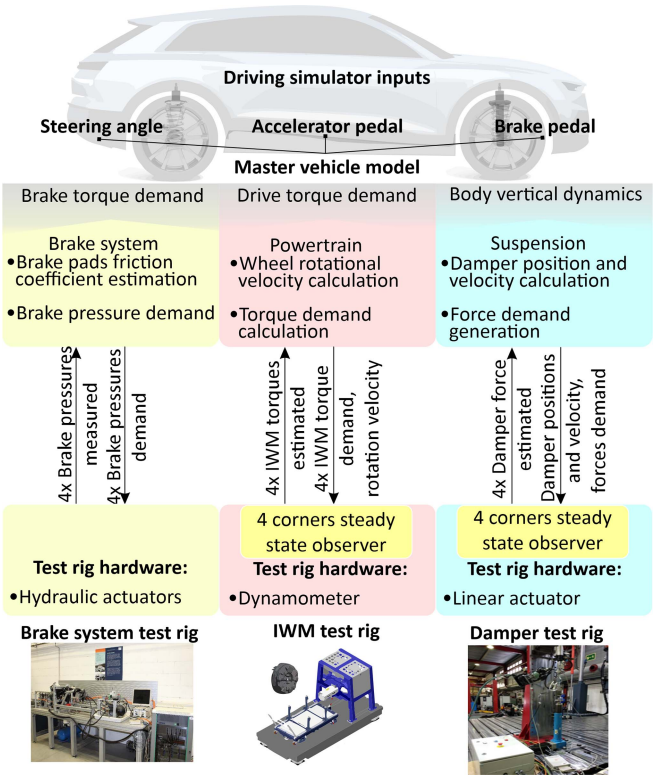

FIGURE 1. Principal XIL architecture.

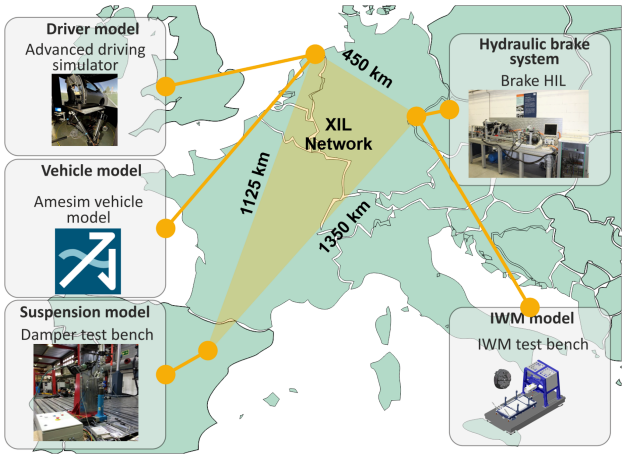

FIGURE 2. Geographically distributed XIL.

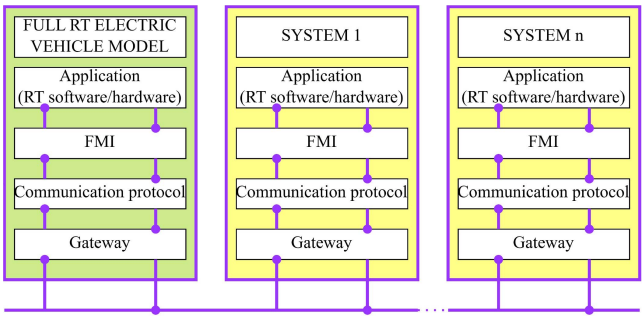

FIGURE 3. General architecture for local and distributed systems.

loss, which should be thoroughly investigated by developing appropriate validation platforms. Various numerical methods to address these challenges are described in the literature, such as a statistical transparency analysis [38], a predictor-based framework [39], robust optimization procedures, i.e. simultaneous perturbation stochastic approximation [40]. With these methods, appropriate compensation mechanisms can be implemented at the software level. Another positive contribution to this issue can be made by advanced telecommunication technologies, new network protocols, and relevant hardware equipment. Overall, this supports the feasibility of remote and distributed XIL testing used for the development of complex systems, such as IMC.

III. FRAMEWORK FOR GEOGRAPHICALLY DISTRIBUTED XIL ENVIRONMENT

For the proposed IMC test, the distributed XIL was built. In Fig. 1, the realized architecture is proposed. On the side of the master EV model is the driving simulator, which replicates the EV dynamics for the driver's perception and receives driver's control actions. The control unit converts the driver inputs into signals that are interpreted by the actuators. For experiment realization, distributed XIL approach was implemented. Test benches were installed in three different locations, as shown in Fig. 2.

The geographical distribution of XIL systems relies on a communication protocol that facilitates long-distance communication. The proposed architecture for both local and distributed systems employs a layered structure. As shown in Fig. 3, the upper layer is the application layer, such as a simulation or testing facility. The second layer involves the Functional Mock-Up Interface (FMI), which maps the exchanged signals. The FMI is an optional layer, as it does not support communication protocols. Therefore, if FMI is unnecessary, signals can bypass it and directly reach the communication protocol layer, which handles the application's native communication protocol. The final layer provides two gateway functionalities. The first function translates communication protocols, such as converting Controller Area Network (CAN) messages to User Datagram Protocol (UDP/IP) datagrams and vice versa. The second function involves routing and transmitting data within a network. A Virtual Local Area Network (VLAN) is used for local communication, while a Virtual Private Network (VPN) is used for distributed systems. For more detail please refer to [1].

The proposed architecture enables plug-and-play functionality in real-time simulations. It identifies the FMI layer and testing platforms above the communication layer.

To ensure robust operations, the system architecture specification includes specific criteria. Compatibility and interoperability are key for distributed systems to function together, allowing for the efficient exchange of signals and data without additional actions. The proposed architecture requires support for specific interfaces to meet these criteria.

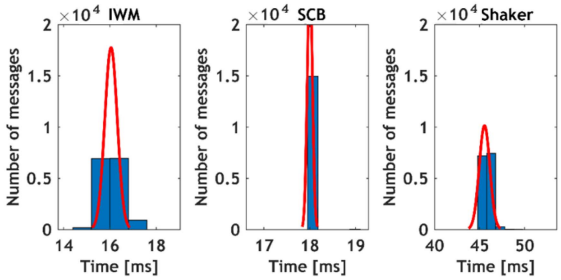

FIGURE 4. Communication delay for IMC testing using distributed XIL.

The reliability of co-simulation and co-testing platforms hinges on the dependable exchange of messages and data. Message loss is an indicator of reliability, and it is measured by the number of messages successfully received over a given time interval. Test scenarios can significantly affect signal number, types, and arrangement. Therefore, a communication protocol must handle all inputs and outputs among distributed systems. However, distributed systems' communication protocols may not always meet real-time requirements, the problem of time synchronization cannot always be solved at the protocol level, so it is necessary to provide an algorithm that takes delay into account and compensates for it. Previous studies show that latency is directly related to the distance between connected clients as well as to the transmission protocol used [1]. The Package Predictive Delay and Dropout Compensation (PPDDC) algorithm, combined with a correction of transferred power in the coupling, has been developed to minimize the round-trip communication time between distributed test environments; for more details, please refer to [33], [41].

To analyze and compare the results of the experiments further, the round-trip time parameter is logged in the geographically distributed XIL simulation environment. It is determined using the time stamp included in each message. The master simulation model compared the simulation time stamp at the simulation moment with the time stamp received from the test bench, with the results of the experiment. The test bench, in return, reprints the time stamp of the message with the received command to the message it sends back with the measurement results.

PPDDC algorithm allowed to split the delay caused by communication as well as the delay caused by the dynamics of the actuators. As a result, latency was analyzed for consistency and absolute value: jitter and delay.

The results of the round-trip time measurements for the different system components are shown in Fig. 4; the number of tests repeated is 15,000 for each case. According to Fig. 4 data, it can be seen that the distance between the various elements of the system increases the delay, while the jitter in the messages remains relatively small. The maximal delay occurred with the AS system; however, it is possible to control the system at a high frequency of 20 Hz.

Modularity is also vital, defined by a system's ability to integrate with other systems within a co-simulation and co-testing environment. In the case of failures, such as communication loss or other errors, the system is being seamlessly transformed from physical to virtual representation, ensuring uninterrupted communication during testing. In the next subsection, the hardware setup is presented.

A. HARDWARE SETUP FOR XIL

To communicate with the brake test bench, the vehicle model requests four pressure signals from the brake system. The sensors on the brake callipers measure the actual brake pressure. The measured values are then transferred to the vehicle model.

The dynamometer with the inverter and the IWM are used to replace the transmission in the EV mathematical model. The sport utility vehicle (SUV) used during the investigation is all-wheel drive, so the sub-system must represent four IWMs. The test bench has a dynamometer and a single IWM. To provide measured values of four IWM torques and rotational speed data to the mathematical model, the application runs a stationary observer on the side of the test bench. The real IWM runs one scenario for testing all IWMs. Developed algorithms accurately replicate the dynamics of all IWMs simultaneously. The input to this test bench is requested torque (calculated based on driver input and demand from the middle-level controller); the output is angular velocity and torque of 4 IWMs.

The suspension test bench allows the replacement of the dampers in the EV mathematical model with AS actuators. This enables accurate investigation of vehicle suspension dynamics and measurement of its parameters. The test bench receives control input to the damper and generates a force that is transmitted to the mathematical model.

Simultaneously, distributed test benches identify whether the actuators can reproduce the demand generated by the controller. An approach based on XIL allows all physical processes in the system to be taken into account with maximum accuracy, taking into account the nonlinearities of actuators and bringing the real-time simulation as close as possible to the dynamics of a real EV.

B. VEHICLE'S MATHEMATICAL MODEL FOR XIL

In this subsection, the high-fidelity EV model is presented, and the IMC is presented and tested using the MIL environment. The vehicle's dynamic model is presented in Fig. 5. The IMC design in this study was carried out for an electric SUV with the following specifications:

- Type of powertrain four wheel drive with IWMs;
- Vehicle mass 2587 [kg];
- Sprung mass 2323 [kg];
- Track width 1.655 [m];
- Center of Gravity (CoG) to front axle distance 1.494 [m];
- CoG to rear axle distance 1.432 [m];
- CoG height 0.484 [m];
- Dimension of the tires 255/55 R19;
- Battery voltage 400 [V];
- Battery capacity 95 [kWh];
- IWM maximum torque 1500 [Nm];

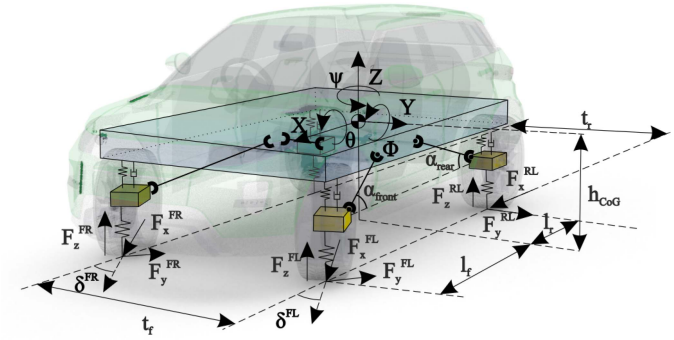

FIGURE 5. Dynamic model of vehicle.

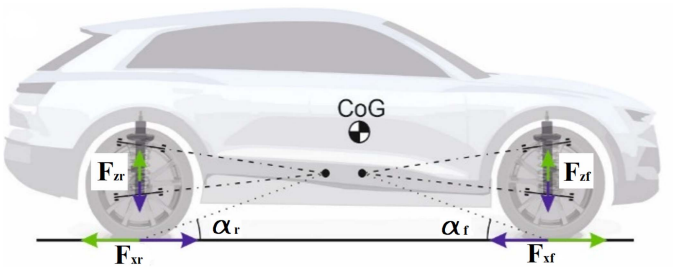

FIGURE 6. Schematic view of vertical force demand.

- Maximum velocity of the EV 181 [km/h].

The EV mathematical model was developed in the Simcenter Amesim simulation environment, validated using experimental data from the proving ground [42], and used in the MIL and XIL environments as a common framework for the operation of all test setups involved.

The equations of motion for the SUV are as follows:

$$\begin{cases} m_s(\dot{V}_x - \dot{\psi}V_y) = \sum F_x = \\ (F_{x,FL} + F_{x,FR})cos(\delta) - (F_{y,FL} + F_{y,FR})sin(\delta) \\ +F_{x,RL} + F_{x,RR} - 1/2\rho C_x A_x {V_x}^2 - \varphi \sum F_z \\ m_s(\dot{V}_y + \dot{\psi}V_x) = \sum F_y = \\ (F_{y,FL} + F_{y,FR})cos(\delta) - (F_{x,FL} + F_{x,FR})sin(\delta) \\ +F_{y,RL} + F_{y,RR} \\ m_s\dot{V}_z = \sum F_z = F_{z,FL} + F_{z,FR} + F_{z,RL} + F_{z,RR} \\ I_{xx}\ddot{\phi} = \frac{t_f}{2}(F_{z,FL} - F_{z,FR}) + \frac{t_r}{2}(F_{z,RL} - F_{z,RR}) \\ +m_s a_y(h_{CoG} - h_r) \\ I_{yy}\ddot{\theta} = -(F_{z,FL} + F_{z,FR})l_f + (F_{z,RL} + F_{z,RR})l_r \\ +m_s a_x(h_{CoG} - h_p) + 1/2\rho C_x A_x {V_x}^2(h_d - h_{CoG}) \\ I_{zz}\ddot{\psi} = ((F_{y,FL} + F_{y,FR})cos(\delta) + (F_{x,FL} + \\ F_{x,FR})sin(\delta))l_f - (F_{y,RL} + F_{y,RR})l_r + \\ ((F_{x,FR} - F_{x,FL})cos(\delta) + (F_{y,FR} - \\ F_{y,FL}) * sin(\delta))\frac{t_f}{2} + (F_{x,RR} - F_{x,RL})\frac{t_r}{2} \end{cases} \quad (1)$$

where m_s is the sprung mass of the EV, I_{xx}, I_{yy}, I_{zz} are the EV moments of inertia. V_x - longitudinal velocity, $\dot{V}_x$ - derivative of longitudinal velocity, V_y - lateral velocity, $\dot{V}_y$ - derivative of lateral velocity, $\dot{V}_z$ - derivative of vertical velocity, $F_{x,i}$ - longitudinal tire force, $F_{y,i}$ - lateral tire force, $F_{z,i}$ - vertical force, δ is steering angle, ρ -air density, C_x - drag coefficient, A_x - frontal cross-section of the EV, φ - rolling resistance of tires, $\ddot{\phi}$ - roll acceleration, $\ddot{\theta}$ - pitch acceleration, $\ddot{\psi}$ - yaw acceleration, h_{CoG} - height of CoG, h_r - the roll center height, h_d - height where drag force is applied, $\dot{\psi}$ - the yaw rate, t_f, t_r - the track width at front and rear axles, l_f, l_r - the distance from the front and rear axle to the EV, a_x, a_y - longitudinal and lateral accelerations. The indices in (1) are designated for the wheels: *FL* - front left, *FR* - front right, *RL* - rear left, and *RR* - rear right.

The vertical force considering the AS is expressed as follows:

$$F_{z,i} = k_i z_i + c_i \dot{z}_i + F_{d_i} \quad (2)$$

where z_i - suspension displacement, $\dot{z}_i$ - the stroke velocity, k_i - the spring stiffness, c_i - the residual damping of the passive components, and F_{d_i} - force from active damper of the wheel $i = FL, FR, RL, RR$.

During acceleration and braking, the vertical load distribution on the front and rear axles changes. This can be mitigated through the use of AS systems. A straightforward method to calculate force demand involves applying the first condition of equilibrium, with longitudinal acceleration as input. However, this approach tends to introduce significant delays when implementing feedback control strategies. A crucial aspect of the proposed approach involves accounting for tire vertical force demand, considering the variations in longitudinal traction and braking forces of the EV. This is achieved using a kinematic method proposed by [13] (refer to Fig. 6). The vertical force demand from the longitudinal force generated by IWM and the brake system on the front and rear axles is expressed as follows:

$$\begin{cases} \delta F_{d,FL} = -tan(\alpha_f)F_{x,FL} = -tan(\alpha_f)(F^{br}_{x,FL} + F^{em}_{x,FL}) \\ \delta F_{d,FR} = -tan(\alpha_f)F_{x,FR} = -tan(\alpha_f)(F^{br}_{x,FR} + F^{em}_{x,FR}) \\ \delta F_{d,RL} = tan(\alpha_r)F_{x,RL} = tan(\alpha_r)(F^{br}_{x,RL} + F^{em}_{x,RR}) \\ \delta F_{d,RR} = tan(\alpha_r)F_{x,RR} = tan(\alpha_r)(F^{br}_{x,RR} + F^{em}_{x,RR}) \end{cases} \quad (3)$$

where $\alpha_{f,r}$ - the angles of the relative rotation of tire-road contact points for the front and rear wheels correspondingly, these angles are defined from SUV suspension kinematics (Fig. 6), $F^{br}_{x,i}$ - braking force, $F^{em}_{x,i}$ - propulsion force from IWM. When the vehicle is accelerating, only the force from the IWM is at play. During braking, several scenarios can occur: *i)* only the IWM is employed to produce negative force, *ii)* both friction brakes and the IWM generate negative forces, and *iii)* only the friction brakes generate negative force (it is a very specific condition not considered in this paper). A portion of the necessary vertical force is computed from 3, while the residual force is determined using a control strategy based on lateral acceleration. To enhance accuracy, terms accounting for drag and rolling resistance forces can be incorporated into (3).

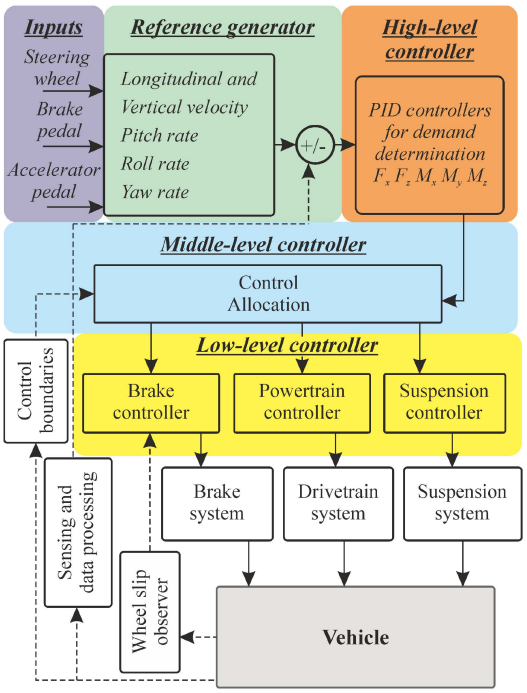

FIGURE 7. Structure of the IMC.

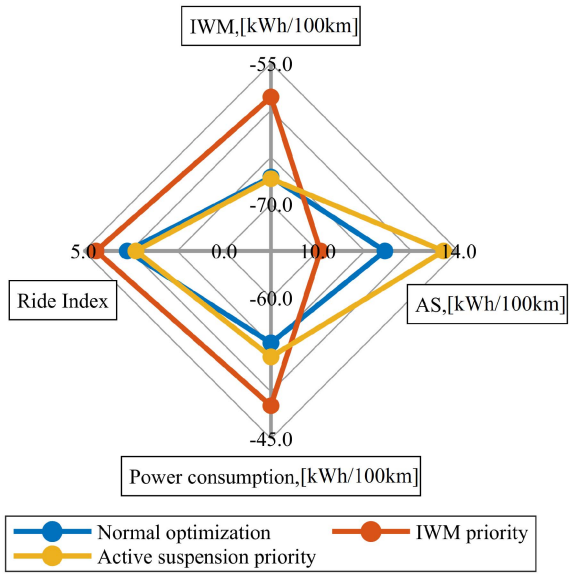

FIGURE 8. Results of SLB maneuver tests.

C. INTEGRATED MOTION CONTROL STRATEGY

The aim of the IMC strategy is to realize an optimal distribution of the control demand between several actuators.

The schematic structure of the IMC is presented in Fig. 7. The responsibilities within the controller layers are distributed as follows. There exist three input parameters: the positions of the steering wheel, braking, and acceleration pedals. These input parameters are sent from the driving simulator to a reference generator, where reference values are determined.

The reference generator uses an EV model that generates reference values based on input parameters and vehicle velocity. In the current case study, the reference generator calculates five reference values $[V_z, \dot{\psi}, \dot{\theta}, \dot{\phi}, V_x]^T$, where $\dot{\theta}, \dot{\phi}$ are pitch and roll rates respectively, V_z and V_x is vertical and longitudinal velocity of the sprung mass. Simultaneously, from the in-vehicle sensors and observers, actual vehicle parameters are received, the rest parameters were described above. The data from the reference generator is utilized to compute the errors.

In the specific scenario being examined, the high-level controller unites five proportional-integral-derivative (PID) controllers, which are required for the development of IMC, which combines a braking system, IWMs, and AS. The controller generates control demand υ_{HL}, which includes: vertical and longitudinal forces, as well as torques for roll, pitch, and yaw:

$$\upsilon_{HL} = \begin{pmatrix} F_{z,dem} \\ M_{x,dem} \\ M_{y,dem} \\ M_{z,dem} \\ F_{x,dem} \end{pmatrix} \tag{4}$$

After calculating the required control demand, the algorithm switches to the middle-level controller, addressing the control allocation task. The primary task is to convert control demands υ_{HL} into four braking torques $T_{br,i}$, $i = FL, FR, RL, RR$, four torques generated by IWMs $T_{em,i}$, and vertical forces $F_{d,i}$ that can be applied as showed in (3). It is possible to distribute the work of each subsystem to achieve key objectives, which may include increasing safety, comfort, or energy efficiency of the electric SUV. The optimal solution is determined by the fixed-point iteration method. As shown in [43] nonlinear relations in the control task could be realized as follows:

$$J_\upsilon = B_\upsilon(\zeta, \upsilon_{CA} - 1)\upsilon_{CA} \tag{5}$$

where B_υ is control effectiveness, ζ defines the significance of the penalization of control agitations, and υ_{CA} is control vector. For the presented control case, the control vector υ_{CA} is expressed as follows:

$$\upsilon_{CA} = \left[F_{d,i}^{CA}, T_{em,i}^{CA,pos}, T_{em,i}^{CA,neg}, T_{br,i}^{CA}\right]^T \tag{6}$$

For the control strategy, there were introduced rule-based distribution between negative torque only from IWM (when the required braking moment is less than IWM could produce $T_{br,i} = T_{em,i}^{neg} < T_{em,i}^{max,neg}$), IWM and friction brakes (when required braking moment is higher than IWM could produce $T_{br,i} = T_{em,i}^{neg} + T_{fr.br,i}^{neg} >= T_{em,i}^{max,neg}$). Here $T_{br,i}$ generated overall negative torque. The control input is presented as follows:

$$\upsilon_{CA} = \left[F_{d,i}^{CA}, T_{em,i}^{CA}, T_{br,i}^{CA}\right]^T \tag{7}$$

The outputs of the control allocation are calculated as follows for the AS:

$$F_{d,i}^{CA} = [F_{d,FL}, F_{d,FR}, F_{d,RL}, F_{d,RR}]^T \tag{8}$$

for IWM:

$$T_{em,i}^{CA} = [T_{em,FL}, T_{em,FR}, T_{em,RL}, T_{em,RR}]^T \tag{9}$$

for braking system:

$$T_{br,i}^{CA} = [T_{br,FL}, T_{br,FR}, T_{br,RL}, T_{br,RR}]^T \tag{10}$$

the dimension of υ_{CA} is 12×1. The matrices B_d, B_{em}, B_{br} calculate the impact of actuators on the vector υ_{CA}. The matrices are defined as follows:

$$B_{as} = \begin{pmatrix} 1 & 1 & 1 & 1 \\ t_l & -t_r & t_l & -t_r \\ -l_f & -l_F & l_r & l_r \\ 0 & 0 & 0 & 0 \\ 0 & 0 & 0 & 0 \end{pmatrix} \tag{11}$$

These parameters are the cost function's variables.

$$B_{em,br} = \begin{pmatrix} \frac{T_{FL}}{R_w} & \frac{T_{FR}}{R_w} & \frac{-T_{RL}}{R_w} & \frac{-T_{RR}}{R_w} \\ \frac{-T_{FL}l_f}{R_w} & \frac{-T_{FR}l_f}{R_w} & \frac{-T_{RL}l_r}{R_w} & \frac{-T_{RR}l_r}{R_w} \\ \frac{T_{FL}l_l}{R_w} & \frac{-T_{FR}t_r}{R_w} & \frac{-T_{RL}t_l}{R_w} & \frac{T_{RR}t_r}{R_w} \\ \frac{T_{FL}t_l\delta}{R_w} & \frac{-T_{FR}t_r\delta}{R_w} & \frac{-T_{RL}t_l}{R_w} & \frac{-T_{RR}t_r}{R_w} \\ \frac{T_{FL}\delta}{R_w tan(\alpha_f)} & \frac{T_{FR}\delta}{R_w tan(\alpha_f)} & \frac{T_{RL}}{R_W tan(\alpha_r)} & \frac{T_{RR}}{R_w tan(\alpha_r)} \end{pmatrix} tan(\alpha_{f,r}) \tag{12}$$

where δ is the steering angle of the front axle. The control efectiveness matrix:

$$B_\upsilon = [B_{as}, B_{em}, B_{br}] \tag{13}$$

the dimension of B_υ is 5×12, finally:

$$B_\upsilon \upsilon_{CA} = \begin{pmatrix} F_z \\ M_x \\ M_y \\ M_z \\ F_x \end{pmatrix} \tag{14}$$

The control allocation problem is formulated as a minimization of allocation error and control actuation, taking into account optimization constraints:

$$\upsilon_{CA} = arg \min_{\upsilon_{lim}^{low} <= \upsilon_{CA} <= \upsilon_{lim}^{up}} (||W_\upsilon (B_\upsilon \upsilon_{CA} - \upsilon_{HL})||_2^2 + \zeta \|W_u \upsilon_{CA}||_2^2) \tag{15}$$

In this task, weighting matrix W_υ is used to set up a priority among generalized forces and torques. W_u corresponds to the weighting matrix for the distribution of demand between chassis subsystems. The parameter ζ defines the significance of the penalization of control actuators.

Optimization is performed in real-time with frequency of 100 Hz. A series of MIL tests were carried out to find a balance between controller performance and energy consumption to define demand distribution between subsystems. The following section presents the results of the simulation.

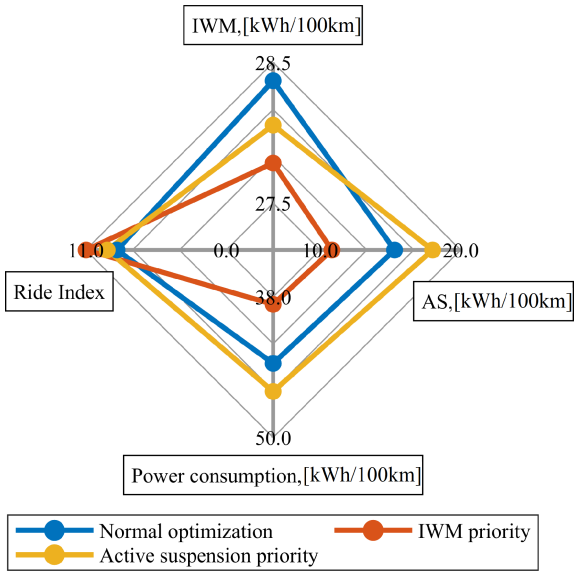

FIGURE 9. Results of DLC maneuver tests.

IV. VALIDATION OF IMC USING GEOGRAPHICALLY DISTRIBUTED XIL

A. DEVELOPMENT OF IMC USING MIL

The following maneuvers were selected to test IMC using the MIL approach:

- Straight line braking (SLB),
- Double lane change (DLC),
- Worldwide harmonized light vehicles test procedure (WLTP), which is the global standard for determining the levels of pollutants and range for EVs.

These maneuvers allow the EV performance to be evaluated using the following key performance indicators (KPIs): *i)* power consumption for each subsystem and *ii)* ride index, weighted RMS of vertical, pitch, and roll accelerations. The weighting procedure is performed following ISO 2631.

To ensure that the proposed IMC strategy had no negative impact on the safety of the EV, the DLC maneuver was performed according to ISO 3888 at the maximum possible velocity at the handling limit.

Different IMC configurations were tested. The first priority for the IWM was granted so that the demanded force was realized primarily by the IWM, and after reaching saturation, the rest of the demand was forwarded to the suspension, and vice versa, when priority was given to the AS.

EV configurations were tuned to provide the most similar ride comfort and driving performance. The results are presented in Fig. 8, Fig. 9, and Fig. 10, showing how the power consumption is allocated for different cases between the systems. Normal optimization in the figures refers to operation in the conventional mode, where control allocation is not applied, and each of the three systems is controlled independently. Power consumption represents the total power used by the system, accounting for AS performance as well as electric motor performance during both propulsion and braking regimes.

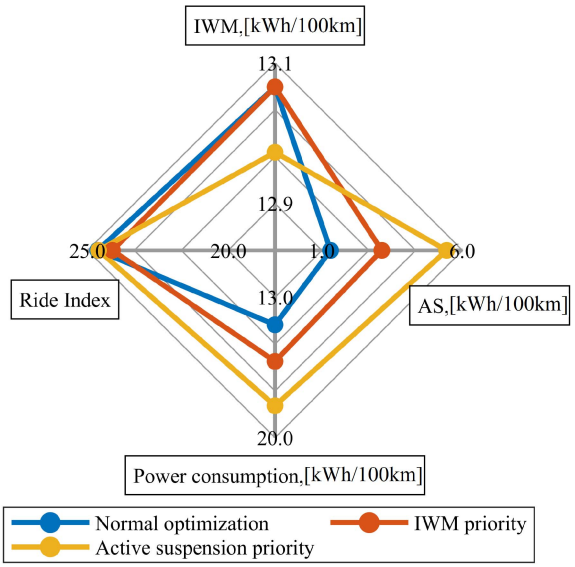

FIGURE 10. Results of WLTP tests.

To perform SLB, the vehicle accelerates up to a velocity of 100 km/h, keeps this velocity up to steady-state behavior, and starts to brake with constant brake pedal actuation corresponding to the 20% of the brake pedal travel. After actuating the brake pedal at the first second of the maneuver, the vehicle drives with an almost constant deceleration of -1 m/s^2.

In Fig. 8 it can be seen that all maneuvers give almost similar results in Ride Index, but the power consumption differs significantly. When the controller prioritizes IWM, the amount of regenerated energy decreases, and the AS consumes less energy. When the suspension has priority in control, the amount of energy recovered by IWM is larger and close to the normal distribution. Still, the power consumption of the suspension is larger than that of normal distribution and IWM priority. In this maneuver, the normal distribution, which corresponds to the same priority for the subsystems, leads to lower power consumption and good result in comfort.

Results of the DLC, presented in Fig. 9, confirm that the amount of power consumed by AS increases when priority is given to it. The difference with SLB is that the priority for IWM lowers the total power consumption. At the same time, the configuration with IWM priority leads to the worst results in the Ride Index. As the duration of the DLC maneuver is short and the maneuver is performed at the EVs handling limit, the data are not sufficient to make a statement about energy consumption. For this purpose, the WLTP cycle was used to evaluate the EVs consumption during long trips. The diagram from Fig. 10 shows the distribution of power between subsystems. The power consumption of the IWM remains relatively stable in absolute terms. Through equal distribution among subsystems, suspension consumption is minimized, resulting in the vehicle with IMC and balanced task distribution among subsystems having the lowest power consumption. Detailed numerical results of the MIL tests are provided in Table 1. During the SLB test, the vehicle generates energy, resulting in negative numerical values for energy consumption (see Fig. 8 and Table 1).

TABLE 1. Comparison of Ride Index and Power Consumption for Different IMC Subsystem Priorities

Equal weight for subsystems				
Maneuver	IWM [kWh/100km]	AS [kWh/100km]	Total EV [kWh/100km]	Ride Index
DLC	28.4	15.3	43.7	8.6
SLB	-67.1	11.9	-53.2	3.4
WLTP	13.0	1.3	14.4	24.6
Priority to the motors				
Maneuver	IWM [kWh/100km]	AS [kWh/100km]	Total EV [kWh/100km]	Ride Index
DLC	27.8	10.8	38.6	11
SLB	-58.6	10.1	-48.5	4.5
WLTP	13.0	3.1	16.1	24.1
Priority to the suspension				
Maneuver	IWM [kWh/100km]	AS [kWh/100km]	Total EV [kWh/100km]	Ride Index
DLC	28.0	18.0	46.0	9.3
SLB	-67.3	13.6	-53.7	3.1
WLTP	12.9	5.4	18.4	24.6

The developed controller fully integrates three active chassis systems and allows for tuning responses tailored to the driving conditions. Given that the proposed architecture removes a direct connection between driver inputs and actuators, and all driver intentions are implemented through a feedback control strategy, integrating such a solution into the automated driving concept could yield positive outcomes. Additionally, this controller serves as a replacement for auxiliary sub-controllers like wheel slip control, torque vectoring, and others, as they are already considered within the high-level controller or the wheel slip observer, as shown in Fig. 7.

The suggested solution demands considerably more computational resources, calls for more comprehensive fail-safe strategies, and entails a more elaborate tuning process. In this context, the XIL approach, facilitating testing of the proposed architecture on actual hardware, can offer advantages for the corresponding system design. Additionally, the XIL approach allows for preliminary tuning of the controller, which is essential for vehicle systems integration.

B. IMC TESTING USING GEOGRAPHICALLY DISTRIBUTED XIL

A previously described electric SUV with four independent IWMs, an AS system, and an electro-hydraulic braking system was used to implement and validate the IMC. The reference EV has the same parameters; only its subsystems are

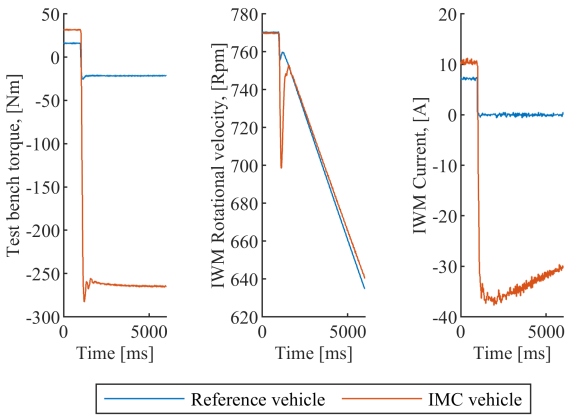

FIGURE 11. Parameters measured by the powertrain test bench during SLB maneuver.

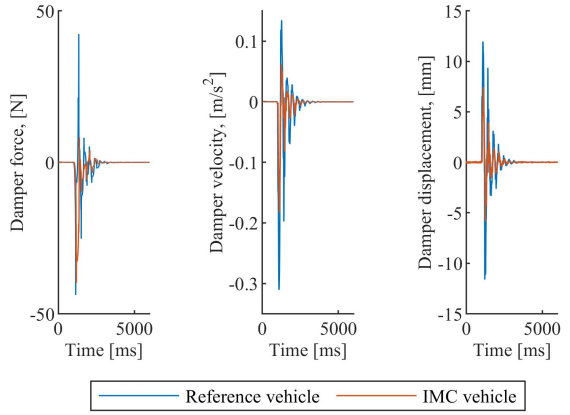

FIGURE 12. Parameters measured by the damper test bench during SLB maneuver.

controlled according to the embedded algorithms. The tests performed are for SLB and DLC maneuvers.

In Fig. 11 and Fig. 12, joint coordination of IWM, brake system, and AS is presented for SLB. It can be seen that the controller periodically actuates torque to dump the vertical oscillations and the pitch rate. According to this test, it can be concluded that the developed IMC brings a positive effect in terms of driving comfort and safety for the braking maneuver.

To study the effect of the proposed IMC on lateral vehicle dynamics, a DLC maneuver has been performed, Fig. 13. During the DLC maneuver, the vehicle is rapidly shifting to a neighboring lane and returning straight back. This can simulate a collision avoidance situation and allows the evaluation of vehicle dynamics in a critical driving case. To demonstrate the IMC effect for a more critical situation, the DLC maneuver has been performed at 85 km/h. A lower speed maneuver does not allow the vehicle to reach its performance limits, and the controller's ability to fully control the vehicle may seem insignificant. At a higher velocity of 85 km/h, the reference vehicle does not pass the maneuver. The IMC operation, which takes into account the vehicle's operating limits, desired yaw rate, and actuator constraints, allows the vehicle to remain stable.

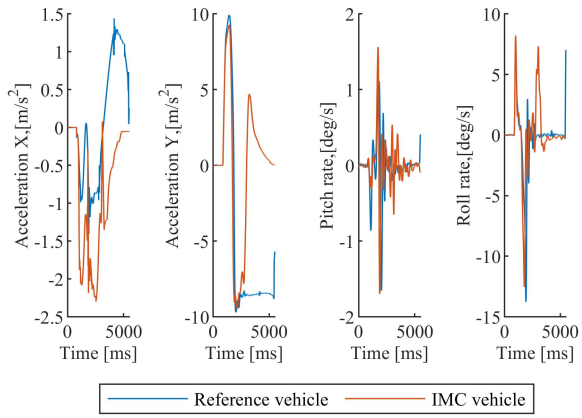

FIGURE 13. Results for DLC maneuver 85 km/h.

TABLE 2. KPI for Safety and Comfort

Manoeuvre	Setup	KPI comfort	KPI safety
SLB	Reference	1.30	1.04
	IMC	0.95	0.97
DLC at 85 km/h	Reference	64.7	0.98
	IMC	17.9	1.00

To evaluate the effect of the IMC on EV dynamics, the KPIs were calculated for defined maneuvers. The KPI for comfort is based on ISO 2631, the KPI for safety corresponds to the RMSE value of the wheel load variations. Results are presented in Table 2. To ensure a reliable evaluation, five representative tests were conducted for both reference and IMC scenarios. This number was selected to effectively capture variability while minimizing the influence of the driver's inherently inconsistent actions across runs. Outliers exceeding three standard deviations were excluded to prevent skewing the results. A decrease in the numerical values in Table II indicates that KPIs for IMC evaluation would correspond to an improvement in the quality/performance of the maneuver about the specific vehicle feature (comfort or safety).

It can be seen that during the SLB maneuver, the KPI for comfort shows an improvement of more than 26%. The KPI for safety hasn't changed significantly, with an improvement of about 7%. In contrast, during the DLC maneuver, the situation was rather different. The KPI for comfort improved by 3.6 times. However, the KPI for safety showed a slight decrease of about 1%. Despite this decrease, the maneuver was completed successfully, whereas a vehicle equipped with a conventional system failed to pass it entirely. This result demonstrates the effectiveness of the proposed IMC approach and, more importantly, the capability of geographically distributed test environments to address industrial challenges.

V. CONCLUSION

The proposed testing methodology establishes a geographically distributed X-in-the-Loop environment for the development and real-time functional validation of various vehicle

systems. In particular, this framework supports a modular, scalable design approach, enabling seamless integration of Hardware-in-the-Loop test benches and other test setups for vehicle systems and components located in different geographical regions for validating integrated motion control strategies.

A dedicated algorithm to minimize round-trip communication times between distributed test environments, for precise separation of communication delays and actuator dynamics, allowed the realization of a geographically distributed X-in-the-Loop environment. This facilitates the implementation of an effective delay compensation method within the simulation environment, ensuring robust real-time performance even when components are separated by distances exceeding 1,000 km. Future advancements in 5G and 6G communication technologies are expected to further decrease communication delays, enabling research into connecting test rigs over even greater distances. These developments will also support the creation of control algorithms and actuators optimized for operation at higher frequencies.

To demonstrate the feasibility of this approach, a case study is presented involving the development of an integrated motion control system that coordinates three vehicle subsystems: in-wheel motors, a fully active suspension, and an electro-hydraulic brake system. The distributed testing framework enables high-fidelity replication of the vehicle model, integration of multiple geographically located test benches, and the use of a driving simulator to assess controller performance within a complex networked architecture.

Results, obtained by means of the distributed tests, confirm the effectiveness of the proposed controller, showing improvements in both ride comfort and safety-related key performance indicators of the target vehicle. For straight-line braking, the average comfort improvement was more than 26%, and approximately 3.6 times better performance was achieved during a double lane change manoeuvre. Meanwhile, the vehicle with the integrated control was able to execute the manoeuvre at the designated speed. This achievement highlights the potential of integrated motion control for application in automated vehicles, where the driver becomes an occupant, and comfort becomes a critical aspect for reducing motion sickness. A new framework for integrated motion control techniques has been proposed, and the results obtained may serve as a baseline for further research.

VI. DISCLAIMER

Funded by the European Union. Views and opinions expressed are those of the authors only and do not necessarily reflect those of their affiliation organisations and the European Union or European Research Executive Agency. Neither the European Union nor the granting authority can be held responsible for them.

REFERENCES

[1] V. Schreiber et al., "Shared and distributed X-in-the-loop tests for automotive systems: Feasibility study," *IEEE Access*, vol. 6, pp. 4017–4026, 2018.

[2] N. A. Schilke, R. D. Fruechte, N. M. Boustany, A. M. Karmel, B. S. Repa, and J. H. Rillings, "Integrated vehicle control," in *Proc. Int. Congr. Transp. Electron.*, 1988, pp. 97–106.

[3] B. Shyrokau, D. Wang, D. Savitski, K. Hoepping, and V. Ivanov, "Vehicle motion control with subsystem prioritization," *Mechatronics*, vol. 30, pp. 297–315, 2015.

[4] D. Savitski, V. Ivanov, B. Shyrokau, J. De Smet, and J. Theunissen, "Experimental study on continuous ABS operation in pure regenerative mode for full electric vehicle," *SAE Int. J. Passenger Cars- Mech. Syst.*, vol. 8, no. 2015-01-9109, pp. 364–369, 2015.

[5] L. Pugi, T. Favilli, L. Berzi, E. Locorotondo, and M. Pierini, "Brake blending and torque vectoring of road electric vehicles: A flexible approach based on smart torque allocation," *Int. J. Electric Hybrid Veh.*, vol. 12, no. 2, pp. 87–115, 2020.

[6] V. Beliautsou et al., "Validation of integrated EV chassis controller using a geographically distributed X-in-the-loop network," in *Proc. 2022 IEEE Veh. Power Propulsion Conf.*, 2022, pp. 1–7.

[7] V. Skrickij, P. Kojis, E. Šabanovič, B. Shyrokau, and V. Ivanov, "Review of integrated chassis control techniques for automated ground vehicles," *Sensors*, vol. 24, no. 2, pp. 1–40, 2024.

[8] S. Sato, H. Inoue, M. Tabata, and S. Inagaki, "Integrated chassis control system for improved vehicle dynamics," in *Proc. Int. Symp. Adv. Veh. Control*, 1992, pp. 413–418.

[9] S. D. Daofei Li and F. Yu, "Integrated vehicle chassis control based on direct yaw moment, active steering and active stabiliser," *Vehicle System Dyn.*, vol. 46, no. S1, pp. 341–351, 2008.

[10] M. Yamamoto, "Active control strategy for improved handling and stability," *SAE Trans.*, vol. 100, pp. 1638–1648, 1991.

[11] G. Mastinu, E. Babbel, P. Lugner, D. Margolis, P. Mittermayr, and B. Richter, "Integrated controls of lateral vehicle dynamics," *Vehicle System Dyn.*, vol. 23, no. sup1, pp. 358–377, 1994.

[12] M. Kissai, B. Monsuez, and A. Tapus, "Review of integrated vehicle dynamics control architectures," in *Proc. Eur. Conf. Mobile Robots*, 2017, pp. 1–8.

[13] E. Katsuyama, M. Yamakado, and M. Abe, "A state-of-the-art review: Toward a novel vehicle dynamics control concept taking the driveline of electric vehicles into account as promising control actuators," *Vehicle System Dyn.*, vol. 59, no. 7, pp. 976–1025, 2021.

[14] S. Horiuchi, K. Okada, and S. Nohtomi, "Effects of integrated control of active four wheel steering and individual wheel torque on vehicle handling and stability - A comparison of alternative control strategies," *Vehicle System Dyn.*, vol. 33, no. sup1, pp. 680–691, 1999.

[15] Z. Hu, Y. Liao, J. Liu, and H. Xu, "Investigation of vehicle stability by integration of active suspension, torque vectoring, and direct yaw control," *SAE Int. J. Veh. Dyn., Stability, NVH*, vol. 6, no. 10-06-04-0029, pp. 441–459, 2022.

[16] J. Song, "Integrated vehicle dynamic controls using active rear wheel steering and four wheel braking," *Int. J. Vehicle Syst. Modelling Testing*, vol. 13, no. 1, pp. 26–43, 2018.

[17] S. Kolte, A.K. Srinivasan, and A. Srikrishna, "Development of decentralized integrated chassis control for vehicle stability in limit handling," *SAE Int. J. Veh. Dyn., Stability, NVH*, vol. 1, no. 2016-01-8106, pp. 1–10, 2016.

[18] J. Zhao, P. K. Wong, X. Ma, and Z. Xie, "Chassis integrated control for active suspension, active front steering and direct yaw moment systems using hierarchical strategy," *Vehicle System Dyn.*, vol. 55, no. 1, pp. 72–103, 2017.

[19] Z. Szalay, "Next generation X-in-the-loop validation methodology for automated vehicle systems," *IEEE Access*, vol. 9, pp. 35616–35632, 2021.

[20] J. Ni, J. Hu, and C. Xiang, "Envelope control for four-wheel independently actuated autonomous ground vehicle through AFS/DYC integrated control," *IEEE Trans. Veh. Technol.*, vol. 66, no. 11, pp. 9712–9726, Nov. 2017.

[21] S. Cheng, L. Li, M. -m. Mei, Y. -l. Nie, and L. Zhao, "Multiple-objective adaptive cruise control system integrated with DYC," *IEEE Trans. Veh. Technol.*, vol. 68, no. 5, pp. 4550–4559, May 2019.

[22] H. Liu, C. Liu, L. Han, and C. Xiang, "Handling and stability integrated control of AFS and DYC for distributed drive electric vehicles based on risk assessment and prediction," *IEEE Trans. Intell. Transp. Syst.*, vol. 23, no. 12, pp. 23148–23163, Dec. 2022.

[23] S. B. Lu, S. B. Choi, Y. N. Li, M. S. Seong, and J. S. Han, "Global integrated control of vehicle suspension and chassis key subsystems," *Proc. Inst. Mech. Engineers, Part D, J. Automobile Eng.*, vol. 224, no. 4, pp. 423–441, 2010.

[24] J. He, D. A. Crolla, M. Levesley, and W. Manning, "Coordination of active steering, driveline, and braking for integrated vehicle dynamics control," *Proc. Inst. Mech. Engineers, Part D, J. Automobile Eng.*, vol. 220, no. 10, pp. 1401–1420, 2006.
[25] A. Chokor, R. Talj, M. Doumiati, and A. Charara, "A global chassis control system involving active suspensions, direct yaw control and active front steering," *IFAC-PapersOnLine*, vol. 52, no. 5, pp. 444–451, 2019.
[26] M. Dalboni et al., "Nonlinear model predictive control for integrated energy-efficient torque-vectoring and anti-roll moment distribution," *IEEE/ASME Trans. Mechatron.*, vol. 26, no. 3, pp. 1212–1224, Jun. 2021.
[27] J. Lee and S. B. Choi, "Integrated control of steering and braking for path tracking using multi-point linearized MPC," *IEEE Trans. Intell. Veh.*, vol. 8, no. 5, pp. 3324–3335, May 2023.
[28] B. Tan, B. Zhang, N. Zhang, Y. Chen, and A. Qin, "Integrated control of electronic stability program and active suspension system using a priority-weighting mechanism," *Proc. Inst. Mech. Engineers, Part D, J. Automobile Eng.*, vol. 237, no. 12, pp. 2857–2871, 2023.
[29] A. Tahouni, M. Mirzaei, and B. Najjari, "Novel constrained nonlinear control of vehicle dynamics using integrated active torque vectoring and electronic stability control," *IEEE Trans. Veh. Technol.*, vol. 68, no. 10, pp. 9564–9572, Oct. 2019.
[30] K. Chatrath, Y. Zheng, and B. Shyrokau, "Vehicle dynamics control using model predictive control allocation combined with an adaptive parameter estimator," *SAE Int. J. Connected Automated Veh.*, vol. 3, no. 12-03-02-0009, pp. 103–117, 2020.
[31] Y. Zhang, S. Lu, Y. Yang, and Q. Guo, "Internet-distributed vehicle-in-the-loop simulation for HEVs," *IEEE Trans. Veh. Technol.*, vol. 67, no. 5, pp. 3729–3739, May 2018.
[32] W. Niu, S. Ke, Q. Xiao, M. Behrendt, A. Albers, and T. Zhang, "Transparency of a geographically distributed test platform for fuel cell electric vehicle powertrain systems based on X-in-the-loop approach," *Energies*, vol. 11, no. 9, 2018, Art. no. 2411.
[33] J. Alfonso, J. M. Rodriguez, C. Bernad, V. Beliautsou, V. Ivanov, and J. A. Castellanos, "Geographically distributed real-time co-simulation of electric vehicle," in *Proc. 8th Int. Conf. Control, Decis. Inf. Technol.*, 2022, pp. 1002–1007.
[34] V. Ivanov et al., "Connected and shared X-in-the-loop technologies for electric vehicle design," *World Electric Vehicle J.*, vol. 10, no. 4, 2019, Art. no. 83.
[35] R. German et al., "A flexible cloud-based HIL testing of batteries for various electrified vehicles," *IEEE Trans. Veh. Technol.*, vol. 73, no. 4, pp. 4610–4620, Apr. 2024.
[36] N. Wenxu, K. Song, and T. Zhang, "Analysis of geographically distributed vehicle powertrain system validation platform based on X-in-the-loop theory," SAE Int., Warrendale, PA, USA, Tech. Rep. 2017-01-1674, 2017.
[37] S. Sen, P. L. Evans, and C. M. Johnson, "Multi-frequency averaging (MFA) model of electric-hybrid powertrain suitable for variable frequency operation applied in geographically-distributed power hardware-in-the-loop (GD-PHiL) simulation," in *Proc. IEEE Veh. Power Propulsion Conf.*, 2018, pp. 1–6.
[38] T. Ersal, M. Brudnak, J. L. Stein, and H. K. Fathy, "Statistical transparency analysis in internet-distributed hardware-in-the-loop simulation," *IEEE/ASME Trans. Mechatron.*, vol. 17, no. 2, pp. 228–238, Apr. 2012.
[39] Y. Zheng, M. J. Brudnak, P. Jayakumar, J. L. Stein, and T. Ersal, "A predictor-based framework for delay compensation in networked closed-loop systems," *IEEE/ASME Trans. Mechatron.*, vol. 23, no. 5, pp. 2482–2493, Oct. 2018.
[40] V. Schreiber and V. Ivanov, "Optimization using a shared and distributed X-in-the-loop testing environment," in *Proc. IEEE Veh. Power Propulsion Conf.*, 2021, pp. 1–6.
[41] P. Baumann, O. Kotte, L. Mikelsons, and D. Schramm, "Enhancing the coupling of real-virtual prototypes: A method for latency compensation," *Electronics*, vol. 13, no. 6, 2024, Art. no. 1077.
[42] C. Lehne, K. Augsburg, V. Ivanov, V. Ricciardi, F. Büchner, and V. Schreiber, "Fail-safe study on brake blending control," *SAE Int. J. Adv. Curr. Practices Mobility*, vol. 3, no. 2021-01-0983, pp. 1985–1992, 2021.
[43] A. Hac, D. Doman, and M. Oppenheimer, "Unified control of brake-and steer-by-wire systems using optimal control allocation methods," SAE Int., Warrendale, PA, USA, Tech. Rep. 2006-01-0924, 2006.

VIKTAR BELIAUTSOU received the bachelor's degree in aviation system design and the master's degree in mechanical engineering. He is currently working toward the Ph.D. degree with Working Group on Smart Vehicle Systems, Ilmenau University of Technology, Ilmenau, Germany. His research interests include UAV systems, control engineering, vehicle motion control, VTOLs, and aircraft design.

VIKTOR SKRICKIJ received the Ph.D. degree in transport engineering from Vilnius Gediminas Technical University, Vilnius, Lithuania, in 2014. He is currently the Research Director with Transport and Logistics Competence Centre, Vilnius Gediminas Technical University. His research interests include vehicle dynamics, automated driving, and mobility.

JESÚS ALFONSO received the M.S. degree in industrial engineering and the Master's degree in systems and computer engineering. He is currently a researcher and project manager at the Instituto Tecnológico de Aragón, where he is involved in research and innovation projects. He has contributed to several national and international R&D initiatives, including the European project XILforEV. His research interests include real-time simulation, autonomous control, and robotic mobility.

JORIS GILTAY received the M.Sc. degree from the Delft University of Technology, in 2019. From 2019 to 2022, he was a a Researcher Engineer with Haptic Lab and the Section of Intelligent Vehicles, Department of Cognitive Robotics, Delft University of Technology, Delft, The Netherlands. He is currently a Researcher and Development Engineer with Oceaneering, Utrecht, The Netherlands.

FLORIAN BÜCHNER received the M.Eng. degree from the Ilmenau University of Technology, Ilmenau, Germany, in 2018. He is currently Competence Lead for Virtual Validation with EDAG, Ingolstadt, Germany. His research interests include X-in-the-loop methodologies, vehicle safety, and driver assistance systems.

JOSE ANGEL CASTELLANOS (Senior Member, IEEE) received the M.S. and Ph.D. degrees in industrial electrical engineering from the University of Zaragoza, Zaragoza, Spain, in 1994 and 1998, respectively. He is currently a Professor of systems engineering and automation with the University of Zaragoza. He is in charge of courses in SLAM and control engineering with the Department of Computer Science and Systems Engineering. His research interests include SLAM, autonomous vehicle navigation, and decision-making under uncertainty. Dr. Castellanos was an Associate Editor for IEEE TRANSACTIONS ON ROBOTICS and Editor of the IEEE/RSJ International Conference on Intelligent Robots and Systems and the IEEE International Conference on Robotics and Automation.

BARYS SHYROKAU received the joint Ph.D. degree in control engineering from Nanyang Technological University, Singapore, and Technical University, Munich, Germany, in 2015. He is currently an Associate Professor with the Section of Intelligent Vehicles, Delft University of Technology, Delft, The Netherlands. His research interests include vehicle dynamics and control, motion comfort, and driving simulator technology. He was the recipient of scholarship and awards, such as DAAD, IFAC, FISITA, SAE, SINGA, ISTVS, and CADLM.

VALENTIN IVANOV (Senior Member, IEEE) received the Ph.D. and D.Sc. degrees in automotive engineering from Belarusian National Technical University, Minsk, Belarus, in 1997 and 2006, respectively, and the Dr.-Ing. Habil. degree in automotive engineering from Technische Universität Ilmenau, Ilmenau, Germany, in 2017. He was an Assistant, Associate, and Full Professor. In 2007, as a Research Professor, he became Alexander von Humboldt Fellow and in 2008, a Marie Curie Fellow with Technische Universität Ilmenau. He is currently with TU Ilmenau as the Head of the Smart Vehicle Systems Working Group and a Coordinator of several European industrial-academic projects and Marie Skłodowska-Curie Actions. His research interests include vehicle dynamics, electric vehicles, and automotive control systems. Dr. Ivanov is the SAE Fellow, a Member of the Society of Automotive Engineers of Japan, and the Association of German Engineers. He was the recipient of SAE Ralph R. Teetor Educational Award and CADLM Intelligent Optimal Design Prize.